Theor Chem Acc (2011) 130:333–339
DOI 10.1007/s00214-011-0982-0

REGULAR ARTICLE

Adsorption of catechol on a wet silica surface: density functional theory study

Shabeer Ahmad Mian · Xingfa Gao · Shigeru Nagase · Joonkyung Jang

Received: 19 February 2011 / Accepted: 18 June 2011 / Published online: 30 June 2011

Abstract Marine mussel proteins adhere permanently to diverse wet surfaces via their catechol (1, 2-dihydroxybenzene) functionality. To elucidate the molecular mechanism underlying this water-resistant adhesion, we performed density functional theory calculations for the competitive adsorption of catechol and water on a wet silica surface. Results show the energetic spontaneity of the reaction; catechol displaces water molecules and adheres directly to the surface. This result was subsequently corroborated by our molecular dynamics simulation.

Keywords Mussel adhesion · Catechol · Silica · Water · Density functional theory

Dedicated to Professor Shigeru Nagase on the occasion of his 65th birthday and published as part of the Nagase Festschrift Issue.

Electronic supplementary material The online version of this article (doi:10.1007/s00214-011-0982-0) contains supplementary material, which is available to authorized users.

S. A. Mian · J. Jang (✉)
Department of Nanomaterials Engineering,
Pusan National University, Miryang 627-706,
Republic of Korea
e-mail: jkjang@pusan.ac.kr

X. Gao
Department of Physics, Applied Physics, and Astronomy,
Rensselaer Polytechnic Institute, Troy, NY 12180, USA

S. Nagase
Department of Theoretical and Computational Molecular
Science, Institute for Molecular Science, Myodaiji,
Okazaki 444-8585, Japan

1 Introduction

An adhesive that is capable of sticking to wet surfaces has numerous potential applications including surgical tissue adhesives, dental cement, ship building, and underwater construction [1]. The synthesis of a moisture-resistant adhesive is elusive because of the water layers blocking direct contact with the surface. However, marine mussels naturally overcome this obstruction and adhere to virtually any wet surface, even under saline and tidal conditions [2–4]. This fact has triggered extensive efforts to elucidate the mussel adhesion mechanism. Mussel adhesive proteins (MAPs) are known to have an unusually high content of 3,4-dihydroxy-L-phenylalanine (L-DOPA) [5–7]. The consensus view is that the catechol functionalities (1, 2-dihydroxybenzene) of L-DOPA anchor MAPs on the surface to which they adhere to [8, 9]. The oxidized catechol (quinone) is responsible for the subsequent cross-linking of MAPs (curing) necessary to form a matrix of adhesion [10, 11].

It remains unclear how catechol displaces the pre-adsorbed water molecules and establishes firm adhesion, especially onto a hydrophilic surface that has strong affinity for water. We recently calculated the binding energy of catechol on an amorphous silica using density functional theory (DFT) [12]. Catechol adhered to the silica more strongly than water. The versatility of catechol adhesion is attributable to the torsion of its hydroxyls (OHs); the OHs and the phenylene ring of catechol, respectively, contributed to adhesion via hydrogen (H) bonds and dispersion interactions. The displacement of the pre-adsorbed water molecules by catechol was not studied in our previous work. A geometry optimization showed that the binding of catechol to the silica surface remains intact after adding water molecules around the

adsorbed catechol. However, this can be attributed to a kinetic bottleneck in the optimization. A definitive proof of the displacement of water by catechol calls for a new approach.

Herein, we simulate the competitive adsorption of catechol and water by explicitly considering the presence of water molecules co-adsorbing with catechol. A hydroxylated silica surface is chosen to model an amorphous silica that is most relevant to the underwater adhesion of mussels. Adopting the procedure reported by Rimola et al. [13], we investigate the energy change involved in the adsorption of catechol on a wet silica surface. The present DFT calculation reveals that catechol prefers direct contact with the surface to being bridged by intervening water molecules. Our molecular dynamics (MD) simulation also illustrates that catechol expels pre-adsorbed water molecules and adheres directly to the surface.

2 Computational methods

We conducted periodic DFT calculations using generalized gradient approximation (GGA) for the exchange correlation functional by application of a modified Perdew–Burke–Ernzerhof (PBE) method [14]. Core electrons were treated using norm-conserving pseudopotentials, following a procedure described by Troullier and Martins [15]. Valence electrons were treated using atomic orbitals at the level of double zeta with polarization (DZP). The mesh cutoff [16] for our atomic orbitals was 5.44 keV. We applied the Monkhorst–Pack scheme [17] with $6 \times 6 \times 1$ k points for sampling the Brillouin zone. We optimized geometries using the conjugated gradient method [18] and by allowing periodic cells to vary. Geometry optimization was taken to be converged if the maximal atomic force is smaller than 0.0001 eV/Å. No symmetry was assumed throughout the calculation. We used the SIESTA package to implement the DFT methods described earlier [16].

The dispersion interaction was incorporated using the empirical method reported by Grimme [19]. The dispersion energy between atoms i and j, E_{ij}^{disp} is given as

$$E_{ij}^{\text{disp}} = \frac{-s_6\left(C_6^{ij}/R_{ij}^6\right)}{1+e^{\left[-20\left(R_{ij}/R_r-1\right)\right]}}. \quad (1)$$

Therein, R_{ij} is the interatomic distance, and s_6 is the global scaling factor depending on the functional used (=0.75 for PBE). In addition, R_r is the sum of atomic radii, and C_6^{ij} is given, respectively, as the geometric mean of dispersive coefficients of atoms i and j. The values of R_r and C_6^{ij} for H, C, O, and Si were referred from an earlier report [19]. After optimizing geometry using the DFT method presented above, we calculated the dispersion energy of the system by summing Eq. 1 over all the interatomic pairs by imposing two-dimensional periodic boundary conditions with the minimum image convention [20]. According to this convention, each atom interacts with all the other atoms (including the periodic images) that lie inside the periodic cell centered at the position of the atom. The present periodic cell has a dimension of 1.49 nm × 1.49 nm × 4 nm (longest along the surface normal direction). Therefore, the cutoff distance for the dispersion interaction is 0.75 nm at least (note there is no single cutoff distance for this convention). This cutoff distance should be large enough considering the short range of the dispersion interaction (the dispersion interaction is typically truncated at a distance of $2.5\,\sigma$, where σ is about 0.3 nm for most atoms). We are aware that the Grimme's method, Eq. 1, was later modified by Ugliengo [21] and by Jurecka [22]. These modifications could not be used, however, because they were designed for functionals and basis sets different from the present ones.

The present silica surface was created by cutting a slab of bulk α cristobalite along the (001) plane. The slab was made of 16 atomic layers along the surface normal direction. It was a 3×3 surface supercell laterally. We terminated each silicon (Si) atom in the top layer with two OHs, thereby generating geminal silanols. The Si atoms in the bottom layer were terminated by H atoms. The total number of atoms was 198. The layer of Si atoms at the bottom was fixed in the geometry optimization. The periodic simulation box length along the surface normal was more than 40 Å to remove the periodicity along that direction.

3 Results and discussion

The silanol density of the present silica surface is 8.1 per nm^2, which is larger than the typical density of amorphous silica: 5 OH per nm^2 [23]. Therefore, the present surface is strongly hydrophilic. In the optimized geometry of the surface, H bonds exist between the silanols and siloxane bridges of the surface (Throughout this work, an O–H interatomic distance of 1–4 Å is assumed to give an H bond.). Both catechol and water firmly adsorbed onto the surface via multiple H bonds with binding energies of 14.2 and 12.2 kcal/mol, respectively [12] (see Figs. S1 and S2 in Supplementary Materials).

Figure 1 presents the geometry denoted as [(Catechol $-0H_2O$)/$25H_2O$/SiO_2], in which catechol adsorbs directly on the surface surrounded by 25 water molecules per unit cell. Catechol forms four H bonds (shown as dashed lines) with the silanols. The OH groups of catechol act as both donors and acceptors of H. The OHs of catechol rotated torsion angles by −14.2 and 81.3° from the phenylene plane (for an

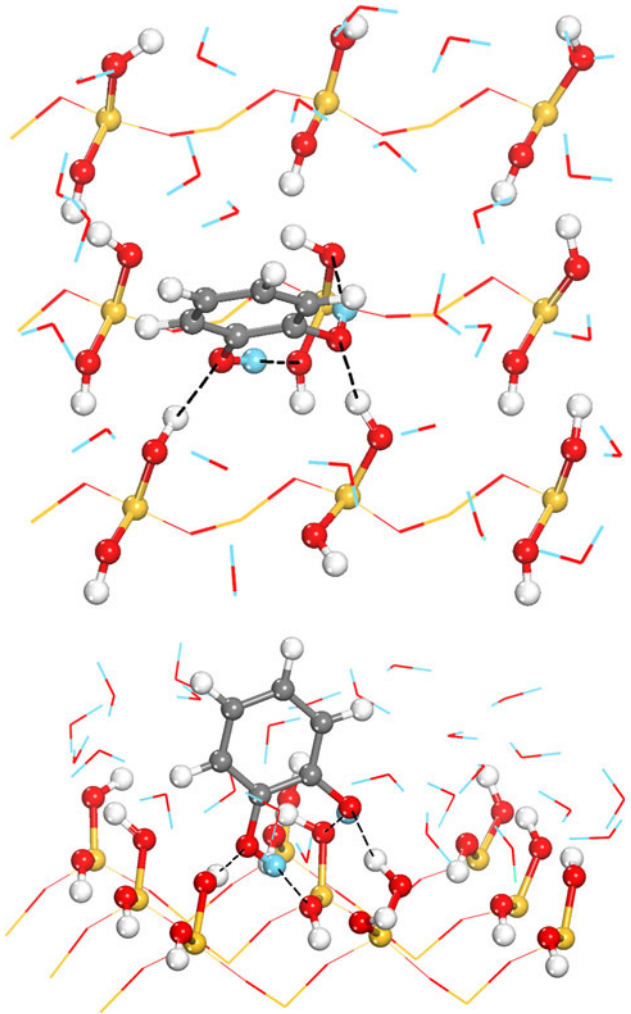

Fig. 1 Catechol adsorbed onto a silica surface together with 25 surrounding water molecules [(Catechol − $0H_2O$)/($25H_2O$/SiO_2]. The optimized geometry is shown in the *top* [*top*] and *side* [*bottom*] views. Only the H bonds between catechol and silanols are marked as *dashed lines*. For visual clarity, other H bonds are not drawn. In this and all subsequent figures, catechol and silanols are shown as *balls* and *sticks*, with the rest shown as *lines*

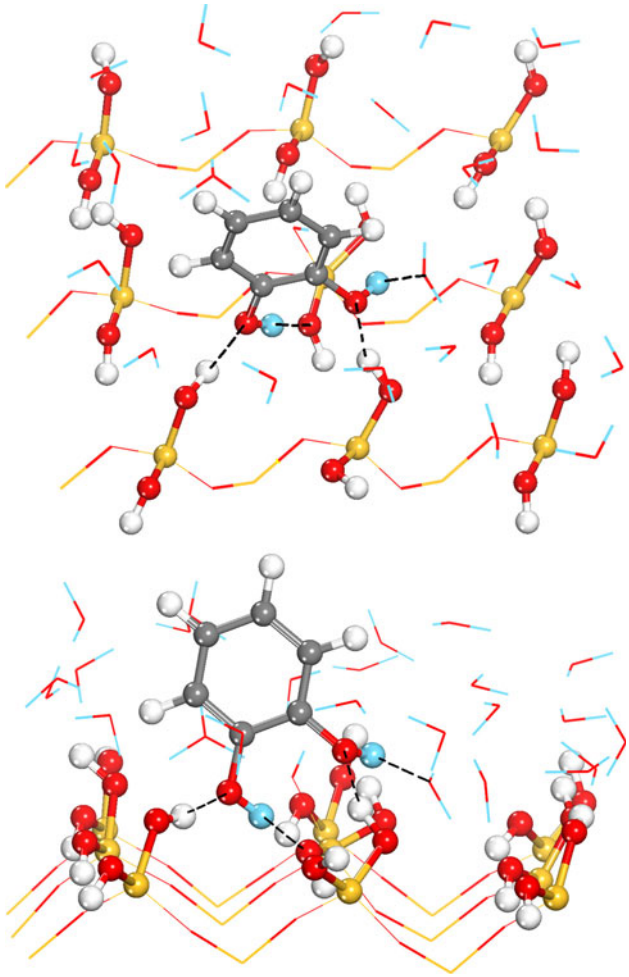

Fig. 2 Adsorption of catechol on a silica surface along with one water molecule interfering in the direct contact of catechol with the surface [(Catechol − H_2O)/($24H_2O$/SiO_2]. The optimized geometry is shown in the *top* [*top*] and *side* [*bottom*] views. Only the H bonds associated with catechol are shown as *dashed lines* for visual clarity

isolated catechol, both OHs lie in the plane of phenylene ring). Water molecules developed H bonds with the silanols and with each other (these are not depicted in Fig. 1 for visual clarity). The adsorption geometry of catechol presented in Fig. 1 is not much different from that of catechol adsorbed with no water molecule. Due to the water molecules intervening between catechol and the silica, the basis set superposition error (BSSE) for the adsorption is not well-defined. In the absence of water molecules, the BSSE for the surface binding of catechol was already reported in our previous paper. There, the BSSE was large (nearly 45% of the binding energy), but the BSSE-corrected binding energy was reasonable, comparing well with experiments and calculations by others.

For the geometry portrayed in Fig. 1, we picked a water molecule weakly bound to the surface (one having the longest H bond with the surface). The selected water molecule was displaced from its original position and placed near one of the OHs of catechol and the silanol forming an H bond with catechol. The following optimization provided the geometry designated as [(Catechol − H_2O)/$24H_2O$/SiO_2], where the displaced water molecule disrupts one of the H bonds between the catechol and the surface (Fig. 2). Catechol lost one H bond with the silanols, but it formed a new H bond with the intervening water molecule (Fig. 2).

Using the geometry of [(Catechol − H_2O)/$24H_2O$/SiO_2], another water molecule weakly bound to the surface was moved close to the OH of the catechol that forms two H bonds with silanols. We then obtained an optimized geometry designated as [(Catechol − $2H_2O$)/$23H_2O$/SiO_2] in which catechol loses all of its H bonds with the silanols,

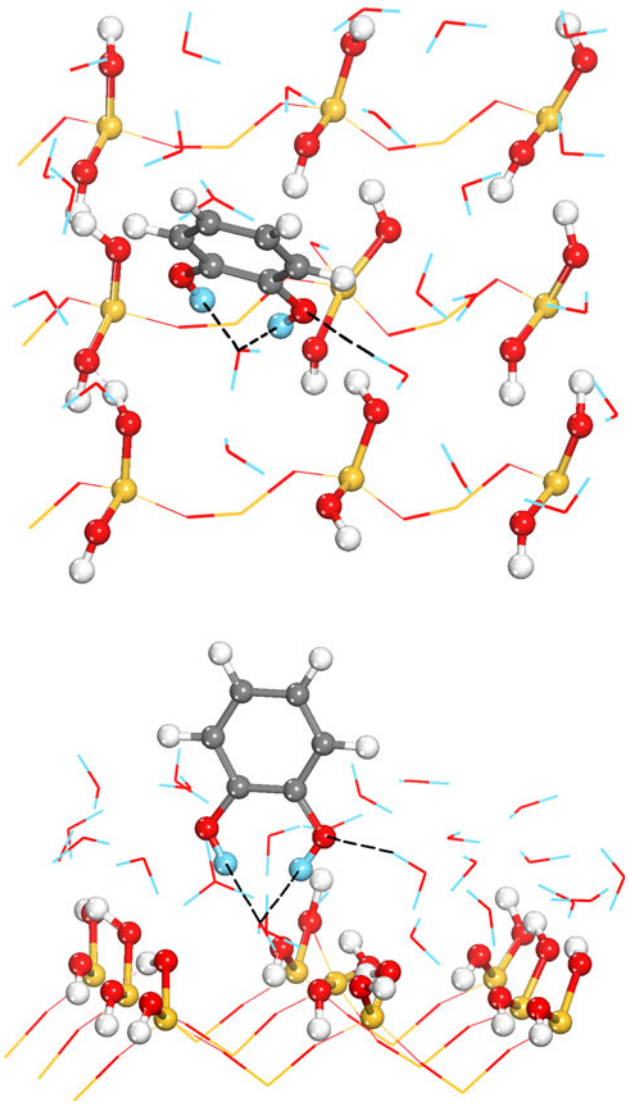

Fig. 3 Adsorption of catechol on a silica surface together with two water molecules intervening in the direct contact of catechol with the surface [(Catechol $-$ $2H_2O$)/($23H_2O/SiO_2$]. The optimized geometry is shown in the *top* [*top*] and *side* [*bottom*] views. Only the H bonds associated with catechol are shown as *dashed lines* for visual clarity

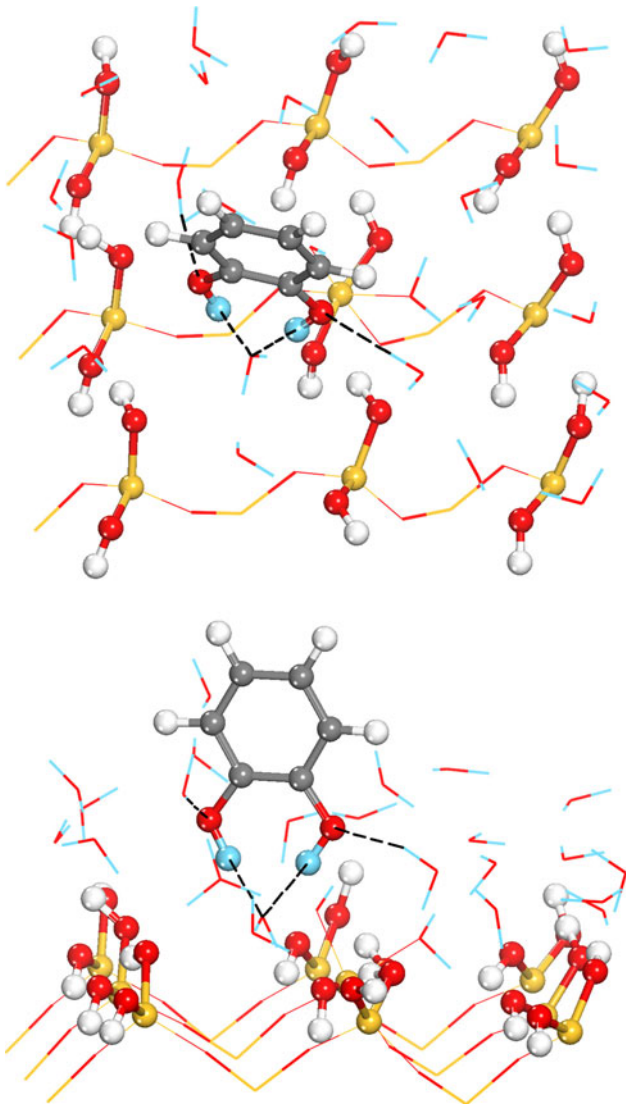

Fig. 4 Adsorption of catechol on a silica surface along with three water molecules interfering in the direct contact of catechol with the surface [(Catechol $-$ $3H_2O$)/($22H_2O/SiO_2$]. The optimized geometry is shown in the *top* [*top*] and *side* [*bottom*] views. Only the H bonds associated with catechol are shown as *dashed lines* for visual clarity

but instead forms three H bonds with two intervening water molecules (Fig. 3).

By displacing a water molecule as above for the geometry [(Catechol $-$ $2H_2O$)/$23H_2O/SiO_2$], we optimized the geometry with three water molecules interfering between catechol and the surface, [(Catechol $-$ $3H_2O$)/$22H_2O/SiO_2$] (Fig. 4). Catechol is farther away from the surface and forms four H bonds with three of the water molecules below it.

The geometries portrayed in Figs. 1, 2, 3, 4 are written collectively as [(Catechol $-$ nH_2O)/($25-n$)H_2O/SiO_2], where n signifies the number of water molecules interfering in the direct contact of catechol with the surface ($n = 0$–3). We now consider the following R1, R2, and R3 reactions, which have one of four geometries of [(Catechol $-$ nH_2O)/($25-n$)H_2O/SiO_2] as products.

$$\text{R1}: \quad [\text{Catechol}/25H_2O] + SiO_2 \rightarrow [(\text{Catechol} - nH_2O)/(25-n)H_2O/SiO_2] \tag{2}$$

$$\text{R2}: \quad \text{Catechol} + [25H_2O/SiO_2] \rightarrow [(\text{Catechol} - nH_2O)/(25-n)H_2O/SiO_2] \tag{3}$$

$$\text{R3}: \quad [\text{Catechol}/25H_2O] + [25H_2O/SiO_2] \rightarrow [(\text{Catechol} - nH_2O)/(25-n)H_2O/SiO_2] + 25H_2O \tag{4}$$

In the R1 reaction, the catechol solvated by 25 water molecules, written as [Catechol/$25H_2O$], adsorbs onto the

Table 1 Energies of the three reactions in which catechol is adsorbed onto a wet silica surface, producing one of four geometries shown in Figs. 1, 2, 3, 4 as a product, ΔE_{R1}, ΔE_{R2}, and ΔE_{R3}

Geometry of product[a]	$-\Delta E_{R1}$	$-\Delta E_{R2}$	$-\Delta E_{R3}$	ΔE_{rel}
[(Catechol − $0H_2O$)/($25H_2O$/SiO_2]	112.1 (148.3)	42.1 (58.8)	43.0 (50.3)	0
[(Catechol − $1H_2O$)/($24H_2O$/SiO_2]	98.4 (136.2)	28.4 (46.7)	29.3 (38.2)	13.7 (12.1)
[(Catechol − $2H_2O$)/($23H_2O$/SiO_2]	91.5 (126.5)	21.5 (37.0)	22.4 (28.4)	20.6 (21.8)
[(Catechol − $3H_2O$)/($22H_2O$/SiO_2]	79.2 (116.1)	9.2 (26.5)	10.1 (18.0)	32.9 (32.3)

The relative energies ΔE_{rel}s of these four geometries are also listed. The numbers in parentheses are obtained by including the dispersion. All values are presented in units of kcal/mol

[a] Geometries are shown in Figs. 1, 2, 3, 4

bare surface, SiO_2, and forms one of the geometries given as [(Catechol − nH_2O)/(25 − n)H_2O/SiO_2]. The first column of Table 1 shows that the reaction energy ΔE_{R1} is exoenergetic irrespective of the number of interfering water molecules n. The solvation (hydration) energy of catechol can be defined as

$$E[\text{catechol}/25H_2O] - E[25H_2O] - E[SiO_2], \quad (5)$$

where E[Catechol/$25H_2O$], E[$25H_2O$], and E[SiO_2], respectively, are the energies of catechol surrounded by 25 water molecules (as in the R1 reaction), of a droplet of 25 water molecules, and of the bare silica surface. The solvation energy was found to be −8.55 kcal/mol (0.87 kcal/mol without the dispersion interaction).

In the R2 reaction, catechol reacts with a wet silica surface covered with 25 water molecules [$25H_2O$/SiO_2] and produces [(Catechol—nH_2O)/(25 − n)H_2O/SiO_2] as a product. This reaction is relevant to the gas-phase adsorption of catechol onto a wet silica surface. The reaction energies ΔE_{R2}s (listed in the second column of Table 1) are exoenergetic as well. The energy of [$25H_2O$/SiO_2] in the R2 reaction, E[$25H_2O$/SiO_2], was further used to calculate the wetting energy defined as

$$E[25H_2O/SiO_2] - E[25H_2O] - E[SiO_2]. \quad (6)$$

The wetting energy was found to be −98.08 kcal/mol (−69.11 kcal/mol in the absence of the dispersion interaction). We also calculated the adsorption energy of 25 gaseous water molecules by replacing E[$25H_2O$] in Eq. 6 by the energy of 25 isolated water molecules. Such an adsorption energy was found to be −27.95 kcal/mol per water molecule (−24.84 kcal/mol without the dispersion interaction). This value is larger than that calculated for a bilayer of water adsorbed on a α quartz (0001) surface (=−15.00 kcal/mol) [24] and a single layer of ice adsorbed on a β cristobalite surface (=−16.42 kcal/mol) [25].

In the R3 reactions, the catechol solvated by 25 water molecules adsorbs onto a wet silica surface, producing one of the geometries [(Catechol − nH_2O)/(25 − n)H_2O/SiO_2] and a cluster of 25 water molecules. These reactions are most relevant to the underwater adhesion of catechol onto a wet silica surface. Table 1 (third column) portrays the R3 reactions that are energetically favorable ($\Delta E_{R3} < 0$).

The stabilities of the geometries given as [(Catechol − nH_2O)/(25 − n)H_2O/SiO_2] can be estimated by the differences in ΔE_{R3}s denoted as ΔE_{rel}s. Table 1 shows that ΔE_{rel} increases concomitantly with the increased number of interfering water molecules. The catechol directly contacting the surface, [(Catechol − $0H_2O$)/($25H_2O$/SiO_2], is much more stable than the others. The populations of geometries with interfering water molecules, $\exp(-\Delta E_{\text{rel}}/k_BT)$, are virtually zero (less than 10^{-9} at 300 K).

The present DFT is reasonably accurate in its description of H bonds [26, 27], but it misses the dispersion interaction between atoms. Ugliengo et al. reported that the dispersive energy is important in the adsorption benzene-1,4-diol on a hydroxylated silica [21]. Therefore, we estimated the dispersive contributions to the reaction energies above using Eq. 1. The resulting reaction energies including dispersion are listed in parentheses in Table 1. This inclusion of dispersion makes the R1, R2, and R3 reactions even more exoenergetic.

In summary, Table 1 demonstrates that catechol adsorption on a wet silica surface is energetically favorable, irrespective of whether the catechol molecule is isolated or solvated by water. Moreover, it is energetically preferred that catechol displaces any intervening water molecules and contacts directly with the surface. The dispersive contribution is particularly large for the R1 reactions. It is 6.1–36.8 kcal/mol in magnitude. In fact, ΔE_{rel}s are nearly unchanged with the inclusion of dispersion.

By calculating the vibration frequencies of molecules and surfaces, it should be in principle possible to calculate the zero point energy (ZPE) and thermal corrections for the reaction energies above [28, 29]. This calculation, however, is found to be too time consuming to be reported in the present study. Moreover, the ZPE and thermal corrections are presumably small, given that the previous work by others reported thermal corrections of 1–2 kcal/mol for the adsorption of hydrocarbon on a nickel surface [30].

To further confirm the molecular mechanism underlying, this water-resistant adhesion, we conducted an MD

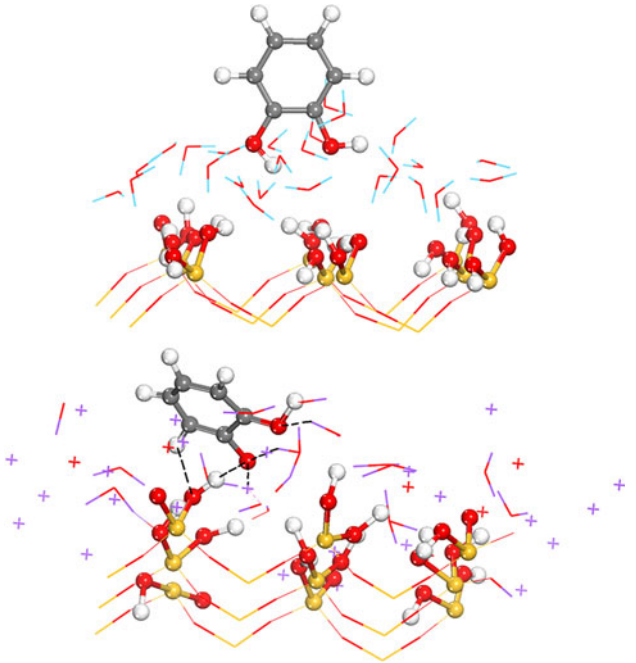

Fig. 5 MD simulation of catechol adsorption on a wet silica surface. The *top panel* shows the initial snapshot where catechol lies on top of 25 water molecules pre-adsorbed onto the surface. The *bottom* shows a snapshot taken at 10 ps. *Crosses* represent protons

simulation for catechol adsorption on a wet silica surface. We placed a catechol molecule on top of the silica surface covered with 25 water molecules (see Fig. S2). A 10 ps long MD trajectory was propagated using the Verlet method with a time step of 1 fs. The forces on atoms were calculated on the fly using the DFT based on the Perdew–Zunger local density approximation (LDA) for the exchange–correlation functional [31]. We used only the Γ point in the integration of the Brillouin zone; the mesh cutoff for atomic orbitals was 2.72 keV. Only the OHs of silanols, water, and catechol are allowed to move in the MD simulation. The initial velocities of atoms were sampled from the Boltzmann distribution at temperature of 300 K. As presented in Fig. 5, catechol indeed relocated the water molecules that had pre-adsorbed onto the surface and finally made direct contact with the surface. We observed that 25 protons are detached from water and the silanols (4 of 18 silanols are oxidized). We ran extensive MD simulations by varying temperature from 0 to 300 K and by using both LDA and GGA methods. The deprotonation occurred in every case, and it always started from one of the surface silanols. We did not find any deprotonation for mutually interacting water molecules or for catechol interacting with water molecules. There have been reports that the surface silanols are acidic (as acidic as vinegar) in the presence of a local strain in geometry [28, 32]. Unlike in our geometry optimization, the MD simulation takes the most of the silica surface to be rigid, and

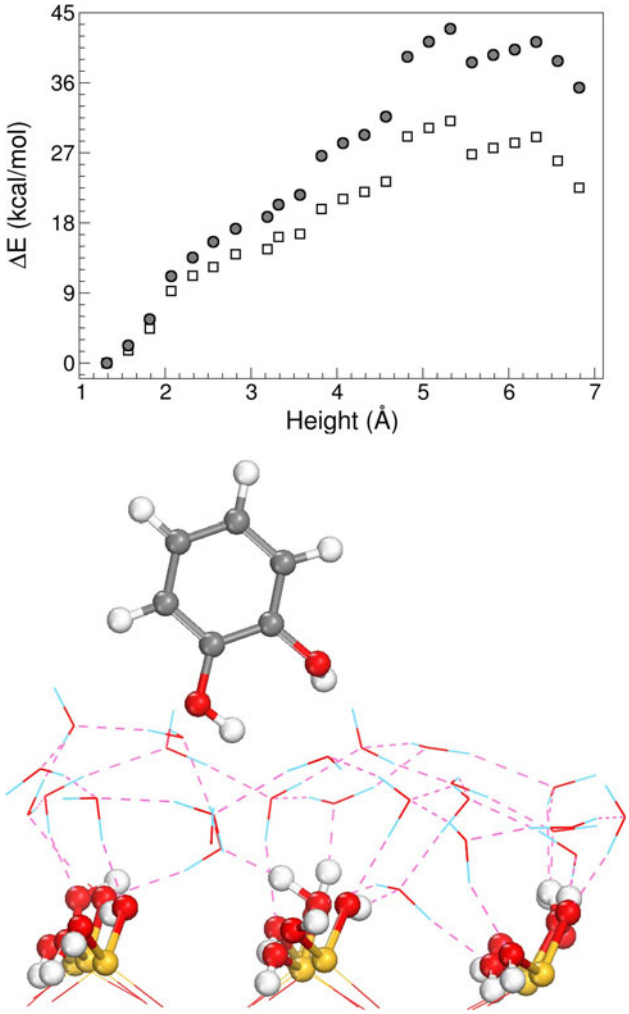

Fig. 6 Energy vs. the height of catechol from the surface [*top*]. The energy ΔE is plotted relative to the energy of the configuration shown in Fig. 1. ΔEs with (*circles*) and without (*squares*) the dispersion interaction are drawn together. *Plotted* is the height of the OH group of catechol closest to the surface measured from the top silicon atoms of the silica. In the *bottom panel*, we draw the configuration for the maximum in ΔE

therefore, the surface silanols can be geometrically strained. This probably makes the surface silanols acidic, leading to their deprotonation. Therefore, the deprotonation presumably arises from the shortcoming of fixing the most of the surface in the present MD simulation.

By considering the various reaction energies defined in Eqs. 2–4, we have shown that catechol displaces the pre-adsorbed water molecules to establish a direct contact with the surface. It would be also interesting to check the potential energy surface (PES) by varying the catechol-surface distance. We constructed such a PES by gradually increasing the height of catechol from the surface starting from the configuration shown in Fig. 1. Plotted in Fig. 1 is the height of the OH group of catechol closest to the surface, and it is measured from the plane of top silicon atoms

of the surface. At each height of catechol, the orientation of catechol was fixed but water molecules are allowed to move for geometry optimization. The energy ΔE plotted in Fig. 6 [top] is relative to the energy of the configuration shown Fig. 1. As shown in Fig. 6 [top], ΔE monotonically increases up to a height of 5 Å and then decreases. Notice ΔEs shown in Fig. 6 are on the same order as ΔE_{rel}s in Table 1. This PES curve also confirms that the displacement of water by catechol is an energetically favorable process. The maximum in ΔE is found at a height where catechol barely touches the water layer below it (the configuration for this maximum is shown in the bottom of Fig. 6). With a further increase in height, catechol loses its contact with the water layer below, and only water molecules adsorb to the surface.

4 Conclusion

In an effort to elucidate the water-resistant adhesion of marine mussels at the molecular level, we performed a DFT study of the competitive adsorption of catechol in the presence of dominant water molecules co-adsorbing onto a hydrophilic silica surface. By analyzing the energetics involved in various cases of the catechol adsorption on a wet silica surface, we showed that catechol adheres directly to the surface by displacing pre-adsorbed water molecules on the surface. This conclusion was confirmed in our MD simulation.

Acknowledgments This research was supported by the Basic Science Research Program through the National Research Foundation of Korea (NRF) funded by the Ministry of Education, Culture, Sports, Science, and Technology (2010-0026100 and 2009-0071412). JJ thanks Prof. Nagase for being supportive and inspirational over the years.

References

1. Ninan L, Monahan J, Stroshine RL, Wilker JJ, Shi R (2003) Biomaterials 24:4091–4099
2. Waite JH (1987) Int JAdhes Adhes 7:9–14
3. Lee H, Lee BP, Messersmith PB (2007) Nature 448:338–341
4. Zhao H, Robertson NB, Jewhurst SA, Waite JH (2006) J Biol Chem 281:11090–11096
5. Guvendiren M, Brass DA, Messersmith PB, Shull KR (2009) J Adhes 85:631–645
6. Wang J, Tahir MN, Kappl M, Tremel W, Metz N, Barz M, Theato P, Butt HJR (2008) Adv Mater 20:3872–3876
7. Weinhold M, Soubatch S, Temirov R, Rohlfing M, Jastorff B, Tautz FS, Doose C (2006) J Phys Chem B 110:23756–23769
8. Yu M, Hwang J, Deming TJ (1999) J Am Chem Soc 121:5825–5826
9. Silverman HG, Roberto FF (2007) Mar Biotechnol 9:66–681
10. AA OOKA, Garrell RL (2000) Biopolymers 57:92–102
11. Monahan J, Wilker JJ (2004) Langmuir 20:3724–3729
12. Mian SA, Saha LC, Jang J, Wang L, Gao X, Nagase S (2010) J Phys Chem C 114:20793–20800
13. Rimola A, Corno M, Zicovich-Wilsonb CM, Ugliengo P (2009) Phys Chem Chem Phys 11:9005–9007
14. Hammer B, Hansen LB, Nőrskov JK (1999) Phys Rev B 59:7413–7421
15. Troullier N, Martins JL (1991) Phys Rev B 43:1993–2006
16. Soler JEM, Artacho E, Gale JD, García A, Junquera J, Ordejon P, Sànchez-Portal D (2002) J Phys Condens Matter 14:2745–2779
17. Monkhorst HJ, Pack JD (1976) Phys Rev B 13:5188–5192
18. Hestenes MR, Stiefel E (1952) Research of the National Bureau of Standards 49:409–436
19. Grimme S (2006) J Comp Chem 27:1787–1799
20. Smith W, Yong CW, Rodger PM (2002) Mol Simul 28:385–471
21. Rimola A, Civalleri B, Ugliengo P (2010) Phys Chem Chem Phys 12:6357–6366
22. Jurečka P, Černý J, Hobza P, Salahub DR (2007) J Comp Chem 28:555–569
23. Du MH, Kolchin A, Cheng HP (2004) J Chem Phys 120:1044–1054
24. Yang J, Wang EG (2006) Physical Review B 73:035406
25. Yang J, Meng S, Xu LF, Wang EG (2004) Phys Rev Lett 92:146102
26. Zhao Y, Truhlar D (2008) Theo Chem Acc 120:215–241
27. van der Wijst T, Guerra CF, Swart M, Bickelhaupt FM (2006) Chem Phys Lett 426:415–421
28. Leung K, Nielsen IMB, Criscenti LJ (2009) J Am Chem Soc 131:18358–18365
29. Tosoni S, Sauer J (2010) Phys Chem Chem Phys 12:14330–14340
30. Mueller JE, van Duin ACT, Goddard WA (2009) J Phys Chem C 113:20290–20306
31. Perdew JP, Zunger A (1981) Phys Rev B 23:5048–5079
32. Hassanali AA, Zhang H, Knight C, Shin YK, Singer SJ (2010) J Chem Theo Comp 6:3456–3471